Ag reflectors: An effective approach to improve light harvesting in Dye Sensitized Solar Cells

Navdeep Kaur, Faizan M. Syed, Jeffrie Fina, Cheng-Yu Lai, and Daniela R. Radu*

Abstract— High-performing and commercially viable dye sensitized solar cells (DSSCs), operable under indirect sunlight illumination, exhibit great potential among current photovoltaic (PV) technologies, however, have smaller light absorption coefficients that hinder their usefulness. In the present work, we have focussed on enhancing the light-harvesting of DSSCs by using silver nanoparticles thin films to improve the light absorption of N719 dye molecules loaded over the active layer of mesoporous TiO₂ (m-TiO₂). The Ag nanoparticles thin films acted as reflectors in the fabrication of DSSCs, which resulted in a power conversion efficiency (PCE) of 6.65% compared to the 5.61% of the standard configuration cells. The effect is ascribed to the increased light absorption ability of DSSCs given the improved reflectivity of the counter electrode (CE) through Ag reflectors, resulting in the reabsorption of reflected light by the sensitized photoanodes. The results were further supported by the reduced resistances at different interfacial layers in the DSSCs, as measured by electrochemical impedance spectroscopy (EIS), thus indicating improved charge transfer kinetics. This work provides insight into the possibility of exploiting Ag nanoparticles in reflectors for improving light harvesting in the PV devices realm.

Index Terms—Ag ink, charge transfer kinetics, dye sensitized solar cells, power conversion efficiency, reflectors

I. INTRODUCTION

In the past few decades, the wide use of non-renewable energy sources like fossil fuels become a universal concern both for harming the environment and, since the demand over availability is increasing drastically, for their rapid depletion. Dye sensitized solar cells (DSSCs), utilizing solar energy, the largest renewable energy source, have been extensively explored for their facile and inexpensive fabrication process, and environmentally friendly nature when compared with other PV technologies [1, 2]. The typical structure of DSSC involves: a mesoporous TiO_2 (m- TiO_2) photoanode sensitized with N719 dye molecules, a I^-/I_3^- redox electrolyte, and a platinum (Pt) counter electrode (CE). Despite the promising features of DSSCs, the lesser absorption of incident sunlight by the dye sensitizers due to the lower reflectivity of transparent Pt CE limits their optimal PV performance. To date,

(Corresponding author: D. Radu; email: dradu@fiu.edu)

various research efforts have been made for the improvement of standard DSSCs via modifying or altering different components. However, factors affecting their PV performance such as the power conversion efficiency (PCE), materials stability, and charge transfer processes do not go hand in hand [3-5]. Considering the significance of standard materials, the external use of reflectors has attracted substantial attention [6-8]. Recently, Ibrahim et al. [9] demonstrated a significant 71.4% enhancement in the PCE of DSSCs using aluminum (Al) foil as reflector, as it contributed not only towards improving the light absorption of sensitized dye molecules via light scattering effect but also escalates the reduction of I_3^- via faster charge transportation. Further, Al reflectors have also been studied by Wu et al. [10] reporting an enhanced PV performance of DSSC with reflectors by 42% relative to the standard cell. Kim et al. [11] investigated the effect of differently patterned i.e., pyramidal, cylindrical, and rectangular molybdenum reflectors in DSSCs and observed the highest PCE increment of 22% for rectangular-shaped Mo reflector-based DSSC. The research finding comparing the PCEs of DSSCs fabricated using metals as reflectors in DSSCs are tabulated in table I.

TABLE I
COMPARATIVE PHOTOVOLTAIC PERFORMANCE OF DSSCS
USING METAL REFLECTORS.

CE Material configuration	<i>PCE</i> (%)	%Change in PCE relative to reference DSSC	Ref.
Ppy/rGO/ITO/Al	1.2	71.4	[9]
Pt/FTO/Al	5.62	42	[10]
Pt/rectangular Mo reflector/FTO	6.81	22	[11]
Pt/FTO/Upconversi on & Ag Nps	7.04	21.3	[12]
Pt/FTO/BaSO ₄	0.008	60	[13]

J. Fina is Ph.D. student in the Department of Mechanical and Materials Engineering Florida International University, Miami, FL 33174 USA. (e-mail: ifina@fiu.edu).

N. Kaur is a postdoctoral associate in the Department of Mechanical and Materials Engineering, Florida International University, Miami, FL 33174 USA (email: nakaur@fiu.edu)

F.M. Syed is a M.S. in Engineering Management and graduate assistant in the Department of Mechanical and Materials Engineering Florida International University, Miami, FL 33174 USA. (e-mail: fsyed011@fiu.edu).

C.-Y. Lai is an Associate Professor in the Department of Mechanical and Materials Engineering Florida International University, Miami, FL 33174 USA. (e-mail: clai@fiu.edu).

D. Radu is an Associate Professor in the Department of Mechanical and Materials Engineering, Florida International University, Miami, FL 33174 USA (email: dradu@fiu.edu)

Present work 6.65 18.53 --

In this work, the PV performance of the DSSCs using standard materials was improved by adding a reflective layer of metallic Ag film at the back of platinum CE. We demonstrated high PCE values, up to 6.65% for the Ag reflector based DSSC, a significant increase from the 5.61% measured for standard DSSC used as a baseline. EIS measurements were conducted to identify the mechanistic underpinnings of the PCE enhancement, supporting the hypothesis that it is caused by a reduction in charge transfer resistances at the interfacial layers.

II. EXPERIMENTAL SECTION

A. Materials and Methods

All the chemicals used in the present work were used as purchased. For synthesizing Ag nanoparticles (NPs), poly(acrylic acid) 25 wt% in water (MW 50,000) and 50 wt% in water (MW 5000) were purchased from Polysciences, Inc., diethanolamine (99%) from Alfa Aesar, and AgNO₃ from Chemsavers. For fabricating DSSCs, fluorine-doped tin oxide (FTO) substrates were procured from Hartford Glass Co., Inc., titanium (IV) isopropoxide (TTIP) and titanium dioxide (TiO₂) paste from Sigma Aldrich, platinum (Pt) paste, Ditetrabutylammonium *cis*-bis(isothiocyanato)bis(2,2'-bipyridyl-4,4'-dicarboxylato) ruthenium(II) (N719) dye, and EL-HSE electrolyte from Greatcell Solar Co. Ltd.

B. Synthesis of Ag ink

Ag NPs were prepared through a procedure adapted from literature [14]. In a typical preparation, poly(acrylic acid) (25 wt% in water, MW = 50,000) (0.18 ml), poly(acrylic acid) (50 wt% in water, MW = 5,000) (0.36 ml), diethanolamine (8 ml) and DI water (5 ml) were added to a 250 ml Erlenmeyer flask and stirred for 15 min at room temperature, to form a homogeneous solution. Further, an amount of 4 ml of AgNO₃ aqueous solution was added dropwise into the above-prepared solution and subjected to 24 h stirring under the same conditions. The resulting dark brown suspension was further ultrasonicated for 1.5 h at 65°C and allowed to naturally cool to room temperature. To collect the NPs, 30 ml ethanol was slowly added (at a 3 ml/min rate) into the above solution, for precipitation, followed by centrifugation. The Ag ink was synthesized by mixing the Ag nanoparticles with nanopure water and ethylene glycol in a 50 ml centrifuge tube, at a ratio of 1:0.55:0.35 (weight ratio) Ag nanoparticles: nanopure water: ethylene glycol. The ink was stirred continuously for 24 h.

C. DSSC fabrication

Photoanode Preparation. FTO substrates were patterned by depositing zinc paste (zinc powder (100 mg) + nanopure $\rm H_2O$ (0.5 ml)) onto the designated area. Once the zinc paste dried, aqueous HCl (18.25% v/v) was poured dropwise on the substrate, causing an exothermic reaction that led to the etching of FTO film on the paste-covered areas on the substrates. The FTOs were further washed with nanopure water. The patterned FTOs were thoroughly cleaned by dipping in individual

beakers, containing soap solution (2% of Hellmanex III in nanopure H₂O), nanopure water, acetone, ethanol, and isopropanol, and ultrasonicated for 15 min each. After every step, the FTO substrates were dried under N₂ flow and finally placed in a UV ozone cleaner for 30 min. A compact layer of TiO₂ (c-TiO₂) was deposited on the pre-annealed FTO substrates, at 450°C, using a spray-pyrolysis method, where 0.4 M solution of TTIP was sprayed on the effective area, further subjected to annealing for 30 min. Over the c-TiO2, m-TiO2 with an effective area of 0.15 cm², was prepared by depositing as procured TiO₂ paste using the doctor blading technique and annealed at 450°C for 30 min, and a clear thin film was obtained. The thickness of c-TiO₂ and m-TiO₂ films are approximately 80 nm and 11.5 µm, respectively, as observed through the cross-sectional FESEM image (Figure 1). The m-TiO₂ thin films were dipped overnight in 0.4 mM solution of N719 dye, and the resultant was the photoanodes of DSSCs.

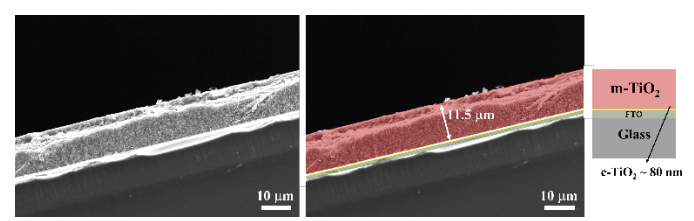


Figure 1. Cross-sectional SEM image of c-TiO₂ and m-TiO₂ films.

Counter Electrodes Preparation. For a comparative investigation, three types of CEs were prepared, first by doctor blading Pt-paste on pre-cleaned FTOs and annealing at 450°C for 30 min, second with Ag ink doctor bladed on the glass side of Pt-CE FTOs and third with doctor blading Ag film on FTO substrate. Figure 2 illustrates the cross-sectional SEM image of Pt and Ag thin film which showed an approximate respective thickness of 450 nm and 7 μ m, respectively. The thickness of c-TiO₂, m-TiO₂, Ag and Pt thin film is still under optimization. Further, the DSSCs were fabricated by assembling photoanodes and CEs in a sandwich-type geometry, along with inserting redox I^-/I_3^- electrolyte in between.

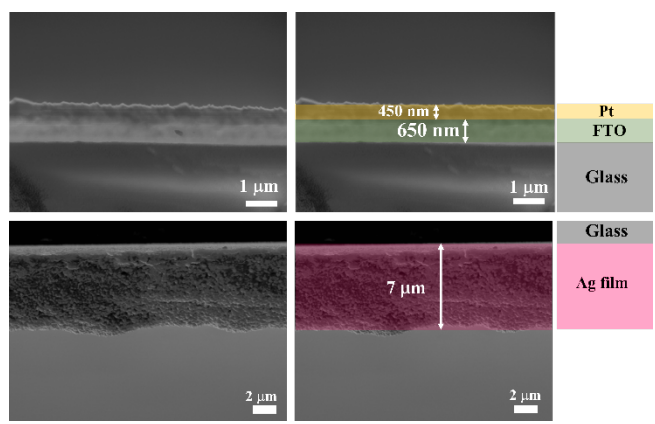


Figure 2. Cross-sectional SEM image of Pt and Ag films.

The structure of the DSSC with and without the Ag thin film reflector addition is illustrated in Figure 3.

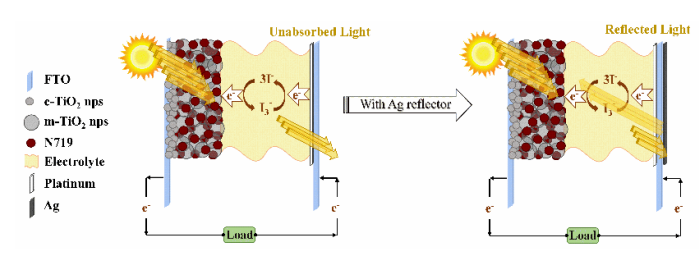


Figure 3. Concept visualization of DSSCs with Ag reflector thin films.

D. Characterization

The PV performance of fabricated DSSCs was tested using an ORIEL LCS- 100^{TM} solar simulator under 1 sun conditions (1.5 G AM) at an intensity of 100 mW·cm⁻², connected to a Keithley source meter (Model 2400). Before the device characterization, the solar simulator was calibrated with a standard silicon cell. EIS measurements were performed on the Ω Metrohm Autolab in a frequency range of 1 Hz to 1 MHz.

III. RESULTS AND DISCUSSION

A. Photovoltaic measurements

The DSSC modified with Ag reflector film showed a PCE of 6.65%, a significant efficiency increase (by 18.53%) from the reference DSSC (5.61%), which is mainly attributed to the increased J_{SC} value from 11.67 mA·cm⁻² to 14.52 mA·cm⁻². Ag CE-based DSSC showed negligible PV performance as Ag NPs are unstable in an iodine-based electrolyte. Figure 4 depicts the current density versus voltage (J-V) curves of the fabricated reference and Ag reflector-based DSSCs along with Ag CEbased DSSC. The derived PV parameters including short circuit current density (J_{SC}) , open circuit voltage (V_{OC}) , fill factor (FF), and PCE are summarized in Table II. The underlying mechanism could be related to the reflective properties of the Ag film, as shown in Figure 3, which materializes in the amplification of the light propagating effect. This further leads to the creation of a large number of photogenerated charge carriers as the incident unabsorbed light is reabsorbed by the sensitized dye molecules, hence resulting in higher J_{SC} and PCE.

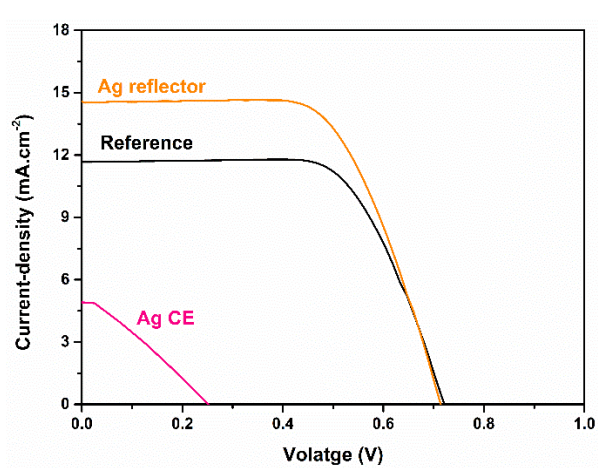


Figure 4. *J–V* curves of fabricated DSSCs without and with Ag

reflector film as well as Ag film as CE.
TABLE II

PV PARAMETERS OF FABRICATED DSSCs WITH DIFFERENT CONFIGURATIONS.

Device Configuration	J _{SC} (mA·cm ⁻²)	Voc (V)	FF	PCE (%)
FTO/c-TiO ₂ /m- TiO ₂ /N719/Electrolyte/Pt/ FTO	11.67	0.72	0.66	5.61
FTO/c-TiO ₂ /m- TiO ₂ /N719/Electrolyte/Pt/ FTO/Ag	14.52	0.71	0.64	6.65
FTO/c-TiO ₂ /m- TiO ₂ /N719/Electrolyte/Ag /FTO	6.55	0.25	0.30	0.49

To investigate the PV performance reproducibility of both reference devices and Ag reflector based DSSCs, ten total devices (five within each configuration) were assembled. It was observed that the PCE within each category of fabricated devices is similar, with a deviation of around $\pm\,0.16$ (Figure 5), which indicates the reproducibility of DSSCs and validates the role of Ag reflector film in producing higher-performance solar cells.

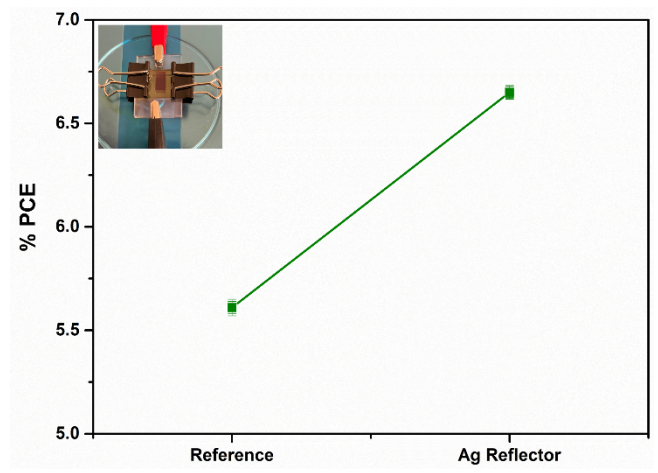


Figure 5. Reproducibility of reference and Ag reflector based DSSCs (The inset shows the image of a typical device).

B. Charge-transfer investigations

To understand the improved PV performance of Ag reflector based DSSCs, the charge transfer mechanism has been estimated from the Nyquist plot (Figure 6) and Bode plots (Figure 7), obtained at respective *Voc*'s under illumination. All the EIS and Bode plot parameters are summarized in Table III. Two distinct semicircles of fabricated DSSCs were observed in the Nyquist curves, where the first semicircle at the higher frequency region corresponds to the charge transfer resistance at the CE and electrolyte interface denoted as RCT, and the second semicircle at the lower frequency region represents the charge transfer resistance (R₁) at photoanode and electrolyte interface. These semicircles were fitted with an equivalent

circuit model $-R_S+Q_1/R_{CT}+Q_2/R_1$, where Q is the constant phase element, Rs is the series resistance of the DSSCs involving FTO's, c-TiO₂, m-TiO₂, electrolyte, Pt CE, and interfaces, and its value is the intercept of the first semicircle at X-axis. R_{CT} and R₁ were obtained from the diameter of the first and second semicircle, respectively. A decrease in the R₁ for Ag reflector DSSC highlights an improvement in the regeneration of dye molecules as well as the electrocatalytic action at CE/ electrolyte interface. Reduced R₁ specifically is the result of the reactions occurring reduced recombination photoanode/electrolyte interface, and hence higher J_{SC} in Ag reflector based DSSC. Rs and RcT were observed to increase in the case of Ag reflector based DSSC in comparison to the reference DSSC, which is attributed to the increase in series resistance of device.

Further, the improved charge transport was confirmed through the electron lifetime at the interfacial layer in DSSCs estimated from Bode plots. The electron lifetime (τ) can be estimated from the characteristic back charge transfer frequency, which is the frequency maxima (f_{max}) of the peak observed in Figure 7, they are inversely proportional to each other as in equation (1):

$$\tau = 1/2\pi f_{max} \tag{1}$$

It is observed that the τ for Ag reflector based DSSC (0.03 ms) is slightly higher than the reference DSSC (0.02 ms) which is in consonance with the higher series resistance of the fabricated devices.

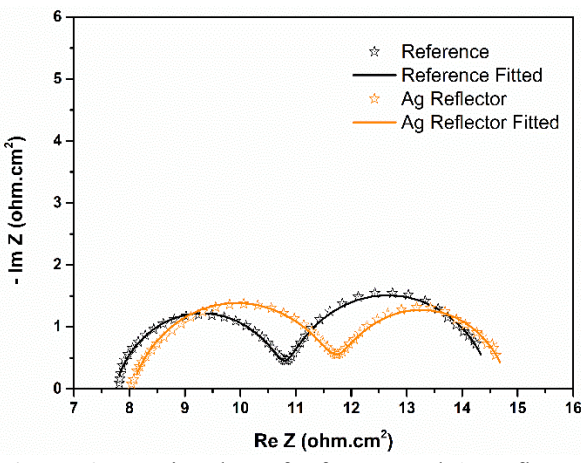


Figure 6. Nyquist Plots of reference and Ag reflector DSSCs fitted with the equivalent circuit model.

TABLE II
EIS PARAMETERS OF FABRICATED DSSCS WITH DIFFERENT
CONFIGURATIONS.

	\mathbf{R}_{CT}	$\mathbf{R}_{\mathbf{S}}$	\mathbf{R}_{1}	τ
Device Configuration	Ω)	Ω)	Ω)	(ms)
	cm ²)	cm ²)	cm ²)	
FTO/c-TiO ₂ /m-	2.97	7.79	3.56	0.02
TiO ₂ /N719/Electrolyte/Pt/FTO				

FTO/c-TiO ₂ /m-	3.21	8.06	2.95	0.03
TiO ₂ /N719/Electrolyte/Pt/FTO/Ag				

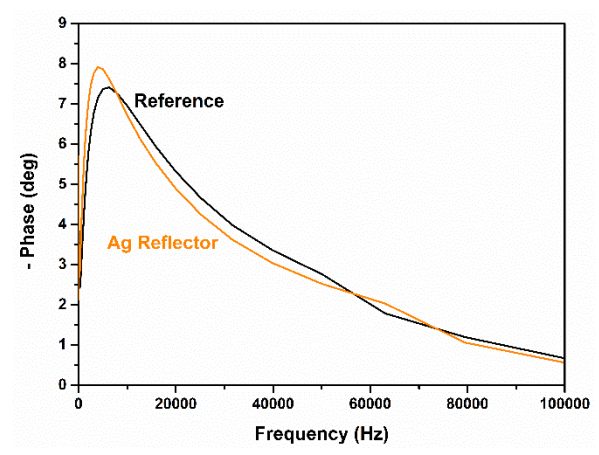


Figure 7. Bode Plots of reference and Ag reflector DSSCs.

IV. CONCLUSION

A simple and elegant approach to improve DSSCs performance using a thin film of Ag as a reflector on Pt CE was successfully demonstrated. A significant improvement in the PCE of Ag reflector based DSSC (6.65%) is observed in comparison to reference DSSC (5.61%) and is attributed to the increased J_{SC}, due to subsequent absorption of unused incident sunlight as it is being reflected towards the photoanode. This leads to further excitation of the dye molecules and aids in generating a large number of photogenerated charge carriers. The EIS measurements confirmed the reduction of the charge transfer resistances at the photoanode/ electrolyte interfacial layer in Ag reflector based DSSC, which indicates a lesser recombination reaction rate and faster catalytic reactions occurring at the electrolyte/CE interface. Hence, the Ag NPsbased thin films could be effectively utilized as reflectors for improving light harvesting in the current DSSC PV technology.

ACKNOWLEDGEMENT

This material is based upon work supported in part by NASA Award #80NSSC19M0201, NASA Award #80NSSC21M0310 and the National Science Foundation under Grant No. DMR-2122078. The authors thank Chen-Yu Chang for SEM imaging.

REFERENCES

- [1] J. Gong, K. Sumathy, Q. Qiao, and Z. Zhou, "Review on dye-sensitized solar cells (DSSCs): Advanced techniques and research trends," *Renewable and Sustainable Energy Reviews*, vol. 68, pp. 234-246, 2017/02/01/2017.
- [2] J. Gong, J. Liang, and K. Sumathy, "Review on dyesensitized solar cells (DSSCs): Fundamental concepts and novel materials," *Renewable and Sustainable Energy Reviews*, vol. 16, pp. 5848-5860, 2012/10/01/2012.
- [3] N. A. Karim, U. Mehmood, H. F. Zahid, and T. Asif, "Nanostructured photoanode and counter electrode

- materials for efficient Dye-Sensitized Solar Cells (DSSCs)," *Solar Energy*, vol. 185, pp. 165-188, 2019.
- [4] A. K. Bharwal, L. Manceriu, C. Olivier, A. Mahmoud, C. Iojoiu, T. Toupance, *et al.*, "Remarkable 8.3% efficiency and extended electron lifetime towards highly stable semi-transparent iodine-free DSSCs by mitigating the in-situ triiodide generation," *Chemical Engineering Journal*, vol. 446, p. 136777, 2022.
- [5] F. Guo, B. K. Narukullapati, K. J. Mohammed, U. S. Altimari, A. M. Abed, Z. Yan, *et al.*, "New material for addressing charge transport issue in DSSCs: Composite WS2/MoS2 high porosity counter electrodes," *Solar Energy*, vol. 243, pp. 62-69, 2022.
- [6] Y.-L. Lee, C.-L. Chen, L.-W. Chong, C.-H. Chen, Y.-F. Liu, and C.-F. Chi, "A platinum counter electrode with high electrochemical activity and high transparency for dye-sensitized solar cells," *Electrochemistry Communications*, vol. 12, pp. 1662-1665, 2010/11/01/2010.
- [7] X. Ma, G. Yue, J. Wu, Z. Lan, and J.-Y. Lin, "A strategy to enhance overall efficiency for dyesensitized solar cells with a transparent electrode of nickel sulfide decorated with poly(3,4-ethylenedioxythiophene)," *RSC Advances*, vol. 5, pp. 43639-43647, 2015.
- [8] L.-P. Heiniger, P. G. O'Brien, N. Soheilnia, Y. Yang, N. P. Kherani, M. Grätzel, et al., "See-Through Dye-Sensitized Solar Cells: Photonic Reflectors for Tandem and Building Integrated Photovoltaics," Advanced Materials, vol. 25, pp. 5734-5741, 2013/10/01 2013.
- [9] I. Ibrahim, H. N. Lim, N. W. K. Wan, N. M. Huang, S. P. Lim, W. Busayaporn, et al., "Plasmonic silver sandwich structured photoanode and reflective counter electrode enhancing power conversion efficiency of dye-sensitized solar cell," Solar Energy, vol. 215, pp. 403-409, 2021/02/01/2021.
- [10] Y.-C. Wu, B.-Y. Lai, C.-t. Chen, S. Yang, and S. Cheng, "Enhancement of light harvesting in dyesensitized solar cells with TiCl4 treatment and high-reflective Pt/FTO/Al counterelectrode," 2010 International Symposium on Next Generation Electronics, pp. 61-65, 2010.
- [11] J.-H. Kim, D.-H. Kim, K.-P. Kim, D.-H. Jeon, and D.-K. Hwang, "Enhancement of the light harvesting efficiency in a dye-sensitized solar cell by a patterned reflector," *Thin Solid Films*, vol. 546, pp. 326-330, 2013/11/01/2013.
- [12] P. Ramasamy and J. Kim, "Combined plasmonic and upconversion rear reflectors for efficient dyesensitized solar cells," *Chemical Communications*, vol. 50, pp. 879-881, 2014.
- [13] A. Zdyb and E. Krawczak. (2021, Organic Dyes in Dye-Sensitized Solar Cells Featuring Back Reflector. *Energies* 14(17).
- [14] B. Y. Ahn, E. B. Duoss, M. J. Motala, X. Guo, S.-I. Park, Y. Xiong, *et al.*, "Omnidirectional printing of flexible, stretchable, and spanning silver

microelectrodes," Science, vol. 323, pp. 1590-1593,